Contribution of NMDA Receptor Channels to the Expression of LTP in the Hippocampal Dentate Gyrus

Zhuo Wang,[1,3,4]* Dong Song,[2,4] and Theodore W. Berger[1,2,3,4]

[1]*Department of Biological Sciences, University of Southern California, Los Angeles, California*
[2]*Department of Biomedical Engineering, University of Southern California, Los Angeles, California*
[3]*Program in Neuroscience, University of Southern California, Los Angeles, California*
[4]*Center for Neural Engineering, University of Southern California, Los Angeles, California*

ABSTRACT: The role of glutamatergic NMDA receptor channels (NMDARs) in the induction of long-term potentiation (LTP) has been well established. In contrast, whether or not NMDARs contribute to the expression of LTP has been an issue of debate. In this study, we investigated the contribution of NMDARs to LTP expression in the hippocampal dentate gyrus (DG) by stimulating perforant path afferents with short bursts of pulses delivered at a moderate frequency (40 Hz), instead of using the traditional protocol of a single stimulus at a low frequency (<0.1 Hz). The synaptic summation provided by the "burst" protocol enabled us to measure the NMDAR-mediated component of synaptic responses (NMDA component), defined as the NMDAR antagonist D-2-amino-5-phosphonovalerate (APV)-sensitive component, in the presence of physiological concentrations of Mg^{2+} (1 mM). Intracellular recordings were obtained from DG granule cells of rabbit hippocampal slices, and excitatory postsynaptic potentials (EPSPs) were measured in terms of the integrated area of their profiles. At 40 Hz, frequency facilitation of the evoked EPSPs was observed. The NMDA component gradually increased during the five-pulse train and frequency facilitation was significantly reduced after the application of APV. We tested the hypothesis that NMDARs undergo potentiation in LTP by comparing the NMDA/non-NMDA ratio of the synaptic responses in control and LTP groups. An increase in the ratio was observed in the LTP group, strongly suggesting potentiation of NMDARs. To infer changes in conductance at individual synapses based on EPSPs recorded at the soma, we constructed a compartmental model of a morphologically reconstructed DG granule cell. The effect on the NMDA/non-NMDA ratio of changes in AMPA and NMDA component synaptic conductance, and of differences in the distribution of activated synapses, was studied with computer simulations. The results confirmed that NMDARs are potentiated after the induction of LTP and contribute significantly to the expression of potentiation under physiological conditions. *Hippocampus 2002;12:680–688.*

KEY WORDS: compartmental model; frequency facilitation; NMDA/non-NMDA ratio

Grant sponsor: Office of Naval Research; Grant sponsor: National Centers for Research Resources (Biomedical Simulations Resource).
*Correspondence to: Zhuo Wang, 403 Hedco Neuroscience Building, University of Southern California, Los Angeles, CA 90089.
E-mail: zhwang@bmsrs.usc.edu
Accepted for publication 10 May 2002
DOI 10.1002/hipo.10104

INTRODUCTION

L-Glutamate is the most widespread excitatory neurotransmitter in the vertebrate central nervous system. Among the three types of ionotropic glutamate receptors, kainate and AMPA receptors, collectively called non-NMDARs, are believed mainly to underlie rapid synaptic transmission, while NMDARs play a more important role in the summation of synaptic responses and the generation of synaptic plasticity (reviewed by Ozawa et al., 1998). NMDARs differ from non-NMDARs in that they have slower kinetics (Lester et al., 1990), are gated by Mg^{2+} in a voltage-dependent manner (Nowak et al., 1984), and are highly permeable to Ca^{2+} (MacDermott et al., 1986). These features allow NMDARs to act as a molecular "coincidence detector" for conjoint pre- and postsynaptic activation. When synapses are activated by high-frequency stimulation (HFS), inward current via non-NMDARs depolarizes the postsynaptic membrane to remove the block of NMDARs by Mg^{2+} (Herron et al., 1986). Ca^{2+} enters through the opened NMDARs and initiates a series of intracellular events that lead to the induction of long-term potentiation (LTP), a long-lasting increase in synaptic strength. LTP is the best studied form of synaptic plasticity believed to underlie certain forms of learning and memory (Berger, 1984; Lynch and Baudry, 1984; Bliss and Collingridge, 1993).

It is well established that HFS induces NMDAR-dependent potentiation of non-NMDAR-mediated synaptic responses. Whether or not potentiation of NMDARs themselves can be induced by HFS has been an issue of debate. LTP can be induced by HFS in pharmacologically isolated NMDARs (Bashir et al., 1991; Xie et al., 1992; but see Kauer et al., 1988; Muller et al., 1988). Potentiation of NMDA component also has been re-

ported in studies in which the NMDA component was isolated only for measurement before and after LTP induction, but not during the LTP induction phase (Muller and Lynch, 1988; Clark and Collingridge, 1995; O'Connor et al., 1995; Xiao et al., 1996; Bayazitov and Kleschevnikov, 2000; but see Muller et al., 1989; Perkel and Nicoll, 1993).

The voltage dependence of NMDARs makes it difficult to measure NMDA component precisely using traditional, low-frequency (<0.1-Hz) single pulse stimulation. In most of the previous studies, the NMDA component was amplified for measurement either by lowering $[Mg^{2+}]_o$ or by voltage-clamping the postsynaptic neuron to a depolarizing potential.

Given the role of NMDARs in inducing synaptic plasticity, it is of great interest to know whether or not NMDARs themselves undergo LTP under physiological conditions. Our laboratory has previously shown that pharmacologically isolated NMDARs can express LTP in the presence of reduced concentrations of Mg^{2+}, or at depolarizing potentials in the presence of normal Mg^{2+} (Xie et al., 1992). In the present study, we further test the possibility that NMDARs express LTP in the presence of normal Mg^{2+} and in response to physiological patterns of afferent stimulation. Considering that bursts of afferent activity are commonly observed in the hippocampus of behaving animals (West et al., 1981; Berger et al., 1983; Wood et al., 2000), we adopted a protocol that uses moderate frequencies of stimulation (40-Hz bursts consisting of five pulses each) to measure the NMDA component (Larson and Lynch, 1988). Temporal summation during the train provides sustained depolarization that removes the Mg^{2+} block of NMDARs. The NMDA component then can be measured by subtracting the complex EPSPs evoked by the 40-Hz trains in the presence of APV (non-NMDA alone) from that in the absence of APV (combined non-NMDA + NMDA). In order to test whether or not NMDARs are potentiated after HFS-induced LTP, we compared the NMDA/non-NMDA ratio of synaptic responses for cells recorded from nonpotentiated (control) slices with that of cells recorded from potentiated (LTP) slices, while maintaining the same level of non-NMDAR activity in both groups of slices. Under the assumption that the non-NMDAR conductance is potentiated by HFS, an unchanged or increased NMDA/non-NMDA ratio would indicate potentiation of the NMDAR conductance, while a substantially decreased ratio would indicate a selective potentiation of the non-NMDAR conductance. We report here that we consistently observed an increase in the NMDA/non-NMDA ratio in the LTP group, strongly suggesting potentiation of the NMDAR conductance.

In addition to changes in synaptic conductance, other factors might contribute to changes in the NMDA/non-NMDA ratio. Assuming that the non-NMDAR conductance at each synapse in the LTP group is greater than that in the control group, a smaller group of synapses would be needed in the LTP group to reach a similar level of non-NMDAR-mediated excitatory postsynaptic potentials (EPSPs). Hence, the stimulus intensity required is lower in the LTP group. Stimuli of lower intensity can be assumed to activate a smaller number of axons that also most likely form synapses closer to each other on the postsynaptic dendritic tree. Increases in the non-NMDAR-mediated depolarization at each synapse might enhance NMDAR activity due to the voltage-dependent blockade of NMDA receptor channels even without potentiation of the NMDAR conductance. To evaluate the potential impact of these factors, a compartmental model was constructed for an anatomically realistic DG granule cell. Simulation results showed that these factors cannot account for the changes in the NMDA/non-NMDA ratio we observed experimentally, justifying the conclusion that NMDARs are potentiated after the induction of LTP and contribute significantly to the expression of potentiation under physiological conditions.

MATERIALS AND METHODS

Electrophysiology

Slice preparation

Hippocampal slices were prepared from New Zealand white rabbits as by Xie et al. (1992). Briefly, transverse hippocampal slices (500-μm thick) were cut with a vibratome and were incubated in medium consisting of (in mM): NaCl, 126; KCl, 3; NaH_2PO_4, 1.25; $NaHCO_3$, 26; glucose, 10; $CaCl_2$, 2; $MgSO_4$, 2, aerated with 95% O_2/5% CO_2. During the recording session, slices were superfused with medium including 100 μM picrotoxin (Sigma) to block γ-aminobutyric acid $(GABA)_A$ inhibition and 1 mM Mg^{2+} at 2.5 ml/min. The temperature was maintained at 31°C throughout all experiments.

Stimulation and recording

A bipolar nichrome stimulating electrode was placed in the middle third of the molecular layer of the DG to activate medial perforant path (MPP) axons. Test pulses with duration of 100 μs were delivered at 0.1 Hz, to monitor synaptic strength. Intracellular recordings were obtained from DG granule cells. Microelectrodes were filled with 2 M KAc (resistance: 100–200 MΩ). A cell was accepted only if its resting membrane potential was greater than −65 mV and if it had an input resistance of >40 MΩ. Small negative current was injected when necessary to keep the membrane potential at −70 mV during testing; normally <0.1 nA of current was needed.

Measurement of the NMDA component

To measure the NMDA component, test pulses were interrupted, and a pair of 40-Hz trains consisting of five pulses each was delivered at a 30-s interval. The duration of each pulse in the train was 100 μs. The test pulses were then resumed, and APV (Tocris) was applied through the bath at 50 μM. At 10 min after the application of APV, another pair of 40-Hz trains was given. An EPSP evoked by a 40-Hz train before APV was defined as a combined response; an EPSP evoked in the presence of APV was defined as a non-NMDA component. The NMDA component was calculated by subtracting the non-NMDA component from the

combined response. The 40-Hz train-induced EPSPs were measured in terms of the integrated area under the EPSP profile. The area of the ith response in the train referred to the area from the onset of the ith stimulus to that of the (i + 1)th (a 25-ms duration). Frequency facilitation was evaluated as the increase of the second through the fifth responses over the first response during the 40-Hz train.

Protocols for the control and the LTP experiments

To compare the NMDA component of the control and the LTP group, we controlled the level of non-NMDAR activity in both groups before measuring the NMDA component. To achieve this goal, we made use of the fact that NMDARs contribute little to the peak amplitude of single pulse-evoked EPSP and used the peak amplitude of single EPSP to approximate the non-NMDA component. For control experiments, stimulation intensity was adjusted within a range of 40–150 μA, to evoke EPSPs of 10-mV peak amplitude for baseline recording. The NMDA component was measured 10 min after baseline recording. For the LTP experiments, stimulation intensity was adjusted to evoke 6-mV EPSPs during baseline recording. After 10 min of baseline, HFS was delivered to induce LTP. HFS consisted of four trains separated by 5-s intervals; each train was composed of 10 pulses delivered at 100 Hz. During HFS, the pulse duration was increased to 200 μs to facilitate LTP induction. The criterion for LTP was a potentiation yielding a peak amplitude ≥10 mV 30 min after the application of HFS. If necessary, stimulation intensity was lowered at this point so that evoked EPSPs had peak amplitudes of 10 mV, equivalent to the amplitude of baseline responses in the control experiments. The NMDA component was then measured. Student's *t*-tests and two-way analysis of variance (ANOVA) with one repeated measure were used for statistical analyses.

Computer Simulations

Model cell morphology and passive membrane properties

Mathematical modeling studies were performed with the NEURON simulator (Hines and Carnevale, 1997). A morphologically realistic granule cell was reconstructed from published anatomical data (Claiborne et al., 1990). Dendritic diameters were estimated according to Desmond and Levy (1984). Spines were simulated on the middle third of the dendritic tree (see Fig. 5A, the region encircled by the solid-line box); spines were distributed over that region uniformly. Each spine consisted of a spine head (diameter 0.55 μm; length 0.55 μm) and a spine neck (diameter 0.1 μm; length 0.73 μm) according to Desmond and Levy (1985). The resting membrane potential was set to −70 mV. Passive membrane properties were chosen after Aradi and Holmes (1999). For the soma, specific membrane resistance R_m = 40,000 Ω-cm^2, specific membrane capacitance C_m = 1 μF/cm^2, and internal resistivity R_i = 210 Ω-cm. For dendritic and spine compartments, R_m = 25,000 Ω-cm^2, C_m = 1.6 μF/cm^2, and R_i = 210 Ω-cm. Here, the dendritic R_m was decreased and C_m increased by a factor of 1.6, to account for those dendritic spines that were not simulated (Aradi and Holmes, 1999). The membrane time constant of the cell was 36 ms, and the input resistance was 310 MΩ. Active conductance was not included in this model (see Discussion).

Model synaptic conductance

Both non-NMDAR and NMDAR conductance were implemented for each model synapse. Each spine was assumed to have only one synapse. The model for the non-NMDAR (AMPAR) conductance was adopted from Kleppe and Robinson (1999):

$$I(t)_{AMPAR} = w \cdot g_{MAX\text{-}AMPAR} \cdot (e^{-t/t_d} - e^{-t/t_r}) \cdot (V - E_{rev\text{-}AMPAR}) \quad (1)$$

where w is the synaptic weight, g_{MAX_AMPAR} is the maximal conductance of AMPARs, t_d and t_r are the decay and rising time constants, and $E_{rev\text{-}AMPAR}$ is the reversal potential of AMPARs. The NMDAR conductance was modeled as two exponentials following Kapur et al. (1997):

$$I(t)_{NMDAR} = w \cdot g_{MAX\text{-}NMDAR} \cdot \frac{e^{-t/\tau_1} - e^{-t/\tau_2}}{1 + \eta \cdot [Mg^{2+}] \cdot e^{-\gamma \cdot V}} \cdot (V - E_{rev\text{-}NMDAR}) \quad (2)$$

where w is the same synaptic weight as in (1), g_{MAX_NMDAR} is the maximal conductance of NMDARs, τ_1 and τ_2 are time constants, η and γ are constants expressing the voltage-dependent block by Mg^{2+}, and E_{rev_NMDAR} is the reversal potential of NMDARs. $E_{rev\text{-}AMPAR}$ and E_{rev_NMDAR} are both 0 mV. The total number of synapses activated is n.

Model parameters

Model parameters were chosen mainly based on original literature and were modified, when necessary, to fit our experimental data. Parameters in the AMPAR model and n were chosen first to fit experimental data. McNaughton et al. (1981) estimated the mean EPSP in DG granule cells resulting from single afferent MPP fiber activation to be 0.1 mV; g_{MAX_AMPAR} was initially chosen so that activation of one synapse with the AMPAR conductance only evoked 0.1 mV EPSP at the soma; n was chosen so that activation of n synapses resulted in 9 mV EPSP at the soma. Once n was chosen, g_{MAX_AMPAR}, t_d, and t_r were further adjusted to fit the simulated non-NMDAR-mediated EPSPs evoked by a single stimulus with the averaged data from control experiments in terms of EPSP area. Parameter values determined in this manner were as follows: n = 70, t_d = 1 ms, t_r = 0.4 ms, g_{MAX_AMPAR} = 10 pS.

A set of synaptic weights, w_1, w_2, w_3, w_4, and w_5, was used to simulate the dynamic changes of presynaptic release during a 40-Hz train; w_1 was set to 1. The parameters w_2–w_5 were chosen so that simulated 40-Hz train-induced non-NMDAR-mediated EPSP fit control data in terms of EPSP area. Thus, parameter values were: w_2 = 1.4, w_3 = 1, w_4 = 0.75, w_5 = 0.55.

Parameters in the NMDAR model were adjusted as necessary so that the simulated train-induced combined response fit control data in terms of integrated EPSP area. The parameters thus chosen were: g_{MAX_NMDAR} = 30 pS, τ_1 = 55 ms, τ_2 = 0.6 ms, η = 0.33 /mM, and γ = 0.14 /mV. A simulated combined response and a non-NMDA component evoked by a 40-Hz train are shown in Figure 4A.

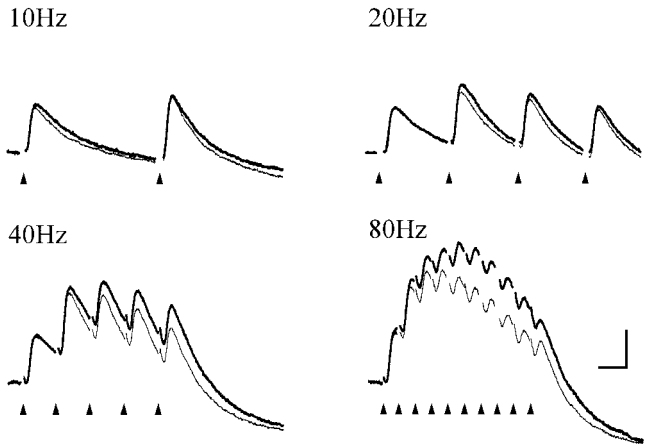

FIGURE 1. Frequency-dependent activation of NMDARs. Representative excitatory postsynaptic potentials (EPSPs) evoked by input trains of different frequencies are shown here. The thick-line traces are EPSPs recorded before the application of APV, defined as combined response. The thin-line traces are EPSPs recorded 10 min after the application of APV, defined as non-NMDA component. The NMDA component was calculated by subtracting the non-NMDA component from the combined. Picrotoxin was not included in the bath in these experiments. Scale bar = 5 mV/20 ms.

RESULTS

Frequency-Dependent Activation of NMDARs

EPSPs recorded from DG granule cells can be separated by bath application of APV into APV-sensitive and APV-insensitive components, defined as the NMDA component and the non-NMDA component, respectively. The threshold frequency required to evoke a significant NMDA component has been reported to be 10 Hz in CA1 pyramidal cells (Collingridge et al., 1988). Blanpied and Berger (1992) have reported that the NMDA component of field potentials recorded in the DG in vivo facilitated markedly in response to frequencies of stimulus input of >20 Hz in the presence of $GABA_A$ antagonist. To find an optimal frequency for measurement of the NMDA component in DG granule cells, we tested the sensitivity of EPSPs to APV for different input frequencies. As shown by responses from a representative experiment in Figure 1, temporal summation of EPSPs during the train was insignificant in response to 10 Hz and 20 Hz, and the NMDA component was small throughout the train. In response to 40 and 80 Hz, significant temporal summation provided sustained depolarization and the NMDA component was reliably evoked in the later part of the train. Because 80-Hz trains could sometimes induce LTP, we chose 40 Hz to measure the NMDA component.

NMDA Component Contributed to Frequency Facilitation

In control experiments, we measured the NMDA component of synaptic responses evoked by 40-Hz trains and investigated the contribution of the NMDA component to frequency facilitation. Frequency facilitation of different components of the synaptic response is shown in Figure 2A. Both the non-NMDA and the NMDA components showed significant facilitation. The non-NMDA component reached its maximal facilitation earlier than the NMDA component. Although the NMDA component had only limited contribution to the combined responses early in the train, the contribution increased later in the train (the average percentages of the NMDA component in the combined response during the train: first pulse 10%, second 21%, third 28%, fourth

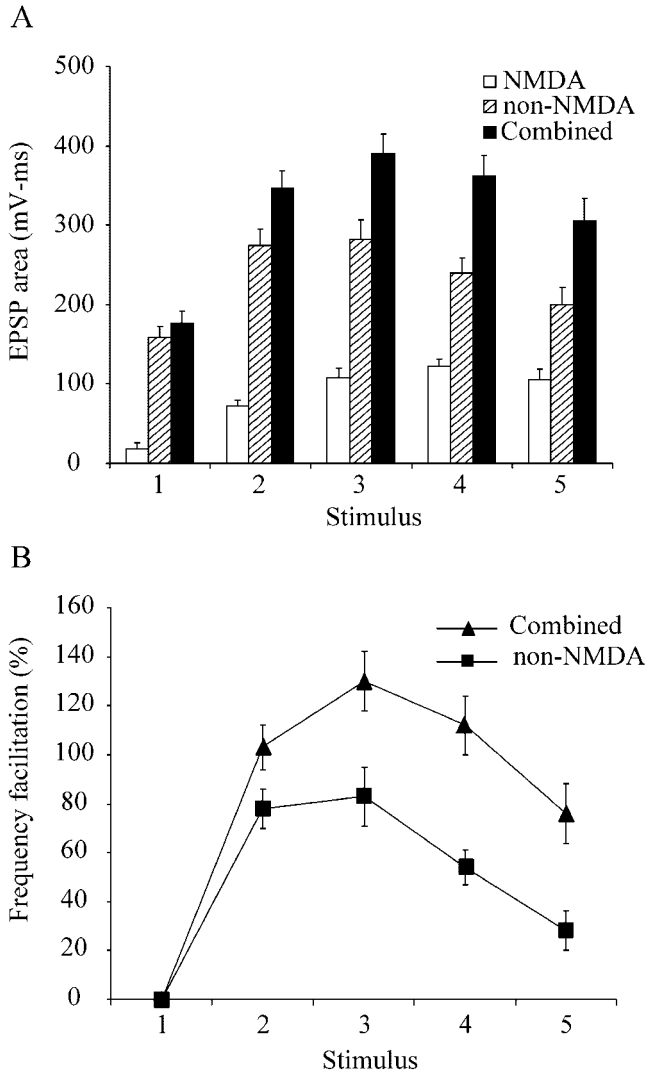

FIGURE 2. NMDA component contributed to frequency facilitation. A: Analysis of different components of excitatory postsynaptic potentials (EPSPs) evoked by 40-Hz trains. Both the non-NMDA and the NMDA component showed significant facilitation during the train. The percentage of the NMDA component in the combined response increased during the train (first: 10%, second: 21%, third: 28%, fourth: 34%, and fifth: 34%). B: Comparison of the pattern of frequency facilitation of the combined response and the non-NMDA component. Frequency facilitation of the combined response was significantly higher than that of the non-NMDA component indicating a contribution of NMDARs to frequency facilitation (second pulse: $P < 0.03$, third: $P < 0.007$, fourth: $P < 0.0004$, fifth: $P < 0.002$, n = 10, two-tailed *t*-test). All values are represented as the mean ±SEM.

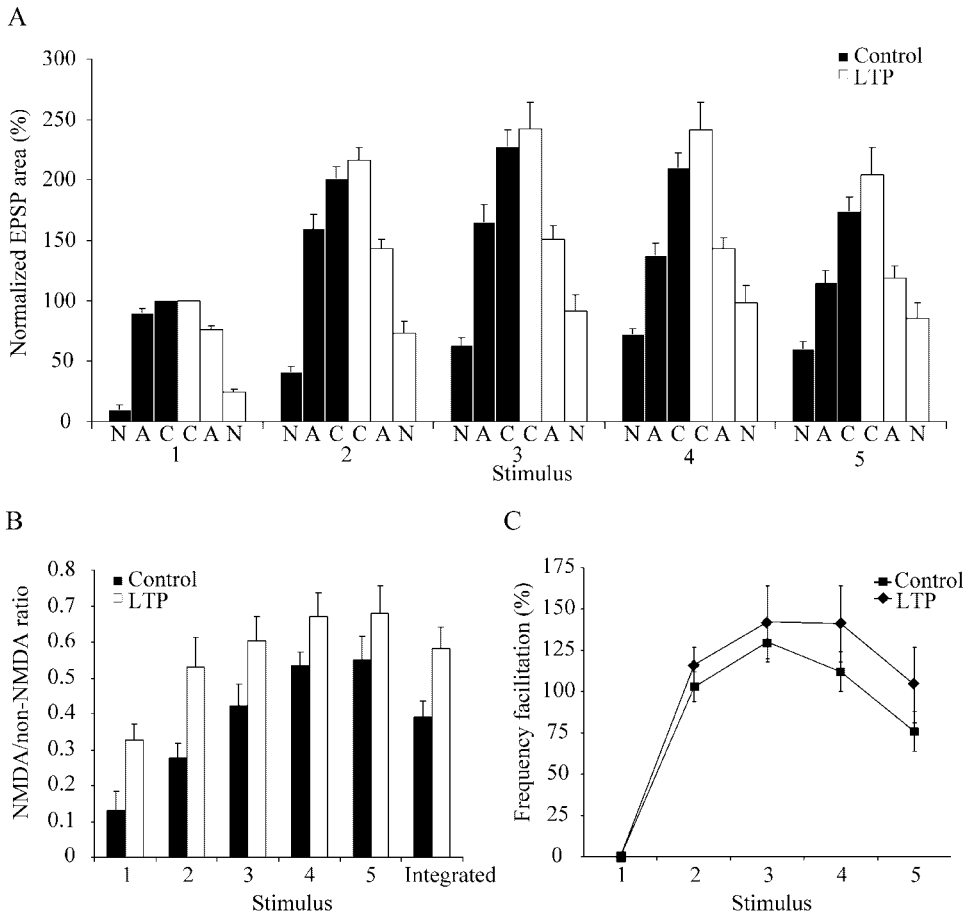

FIGURE 3. Comparison of the NMDA/non-NMDA ratio and the pattern of frequency facilitation of the control and the long-term potentiation (LTP) group. A: Comparison of different components of excitatory postsynaptic potentials (EPSPs) of the control (black) and the LTP (white) group. B: Comparison of the NMDA/non-NMDA ratio. The ratio was significantly higher in the LTP group (n =10, F (1,18) = 6.38, $P = 0.02$, two-way ANOVA). C: Frequency facilitation showed no significant difference between the control and the LTP group (n = 10, F (1,18) = 1.13, $P > 0.3$, two-way ANOVA). All values are represented as the mean ±SEM. A, AMPA (non-NMDA); N, NMDA component; C, combined response.

34%, and fifth 34%). We compared the amplitude of frequency facilitation of the combined response and the non-NMDA component (Fig. 2B). Facilitation of the combined response was significantly greater than that of the non-NMDA component (second: $P < 0.03$, third: $P < 0.007$, fourth: $P < 0.0004$, fifth: $P < 0.002$, n = 10, two-tailed *t*-test). Thus, NMDARs significantly enhanced frequency facilitation.

NMDA/Non-NMDA Ratio Was Increased in the LTP Group

In LTP experiments, we measured the NMDA component after LTP had been induced and tested whether or not the NMDA component is enhanced by the induction of LTP by comparing the NMDA/non-NMDA ratio of the LTP and control group. The non-NMDA component was similar in magnitude for both groups (Fig. 3A). In contrast, the NMDA component showed a significant increase after the induction of LTP. This was reflected by an increased NMDA/non-NMDA ratio in the LTP group (Fig. 3B, n = 10, F (1,18) = 6.38, $P = 0.02$, two-way ANOVA).

Frequency Facilitation Showed no Significant Difference Between Control and LTP Groups

On average, the pattern of frequency facilitation was not significantly different between the control and the LTP group (Fig. 3C, n = 10, F (1,18) = 1.13, $P > 0.3$, two-way ANOVA).

Computer Simulations Show That the NMDA/Non-NMDA Ratio Would be Reduced, and Not Increased, if LTP Were Expressed Selectively by AMPARs (LTP_{AMPA})

We used compartmental neuron modeling to test the effect of a selectively potentiated AMPAR conductance on the NMDA/non-NMDA ratio. Control experiments were simulated (Fig. 4A, number of synapses n = 70). For the LTP scenario, we assumed that LTP is expressed by AMPARs only, denoted as LTP_{AMPA}. We also assumed that the dynamics of presynaptic release are not changed by LTP induction. To estimate the potentiation factor of AMPAR conductance and the total number of activated synapses, we sim-

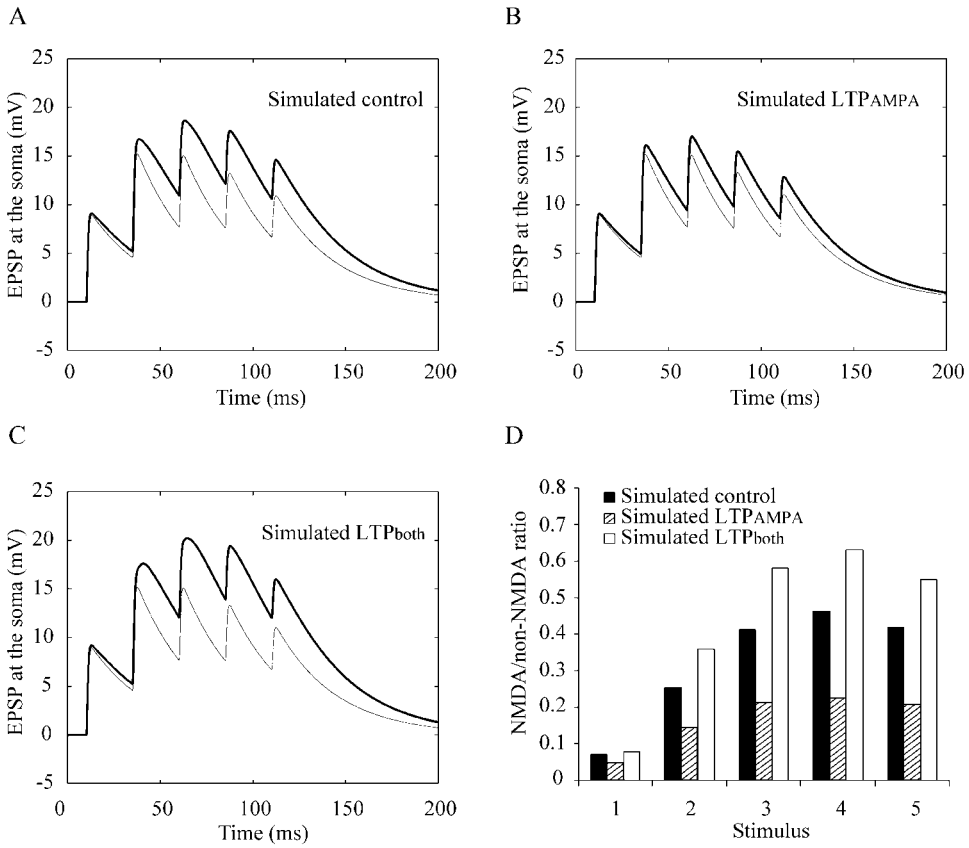

FIGURE 4. Simulation of changes in the NMDA/non-NMDA ratio in two scenarios of long-term potentiation (LTP). A: Simulated control responses. Model parameters were chosen as described in Materials and Methods (number of synapses; n = 70). In B and C as well, thick-line traces represent the combined response; thin-line traces represent the non-NMDA component. B: Simulated responses in the scenario in which LTP is expressed selectively by AMPARs, denoted as LTP_{AMPA}; g_{MAX_AMPAR} was increased by a factor of 1.6, while g_{MAX_NMDAR} remained the same (n = 45). C: Simulated responses in the scenario in which LTP is expressed by AMPARs and NMDARs similarly, denoted as LTP_{both}. Both g_{MAX_AMPAR} and g_{MAX_NMDAR} were increased by a factor of 1.6 (n = 45). D: Comparison of the NMDA/non-NMDA ratio. The ratio decreased in the LTP_{AMPA} scenario; it increased in the LTP_{both} scenario.

ulated an experiment in which the peak amplitude of EPSP evoked by a single stimulus was 6 mV before the induction of LTP and 10 mV afterward. Forty-five synapses were needed to generate a 6 mV EPSP; g_{MAX_AMPAR} was multiplied by a potentiation factor L = 1.6 to generate a 10 mV EPSP after-LTP. The simulation results are shown in Figure 4B. The non-NMDA component was similar to that of the simulated control response (compare the thin-line traces in Fig. 4A,B). The NMDA component, calculated by subtracting the non-NMDA component from the combined response, was much smaller. In contrast to the experimental finding, the NMDA/non-NMDA ratio was approximately 50% lower than the control value (Fig. 4D).

Computer Simulations Show That the NMDA/Non-NMDA Ratio Would be Increased if LTP Were Expressed by Both AMPARs and NMDARs Similarly (LTP_{both})

We simulated another scenario in which AMPAR and NMDAR conductances were potentiated similarly (LTP_{both}). Model parameters were the same as used in LTP_{AMPA} except that g_{MAX_NMDAR} also was multiplied by the potentiation factor L. The NMDA component was greater than the control value (Fig. 4C). Simulation results showed that the NMDA/non-NMDA ratio was increased in this scenario (Fig. 4D). The increase in the ratio was similar to that observed experimentally except for the first response in the train.

Computer Simulations Show That the NMDA/Non-NMDA Ratio Increases, but Is Still Significantly Lower Than the Control Value, in LTP_{AMPA} If the Synapses Cluster Closer Together

The distribution of activated synapses also may have an impact on the NMDA/non-NMDA ratio measured at the soma. After the induction of LTP, activated synapses may be closer to each other since smaller stimulus intensities were used. The previous simulations were all carried out in the region encircled by the solid-line box in Figure 5A. To evaluate the possible effect of the distribution of activated synapses, we redistributed the 45 synapses in LTP_{AMPA} to a smaller region as shown by the dashed-line box in Figure 5A.

This resulted in a slightly reduced non-NMDA component and a slightly enhanced NMDA component in the later phase of the train (Fig. 5B). The NMDA/non-NMDA ratio was higher than the previous simulated LTP_{AMPA} value but was still significantly lower than the control value (Fig. 5C). Given the empirically observed increase in the NMDA/non-NMDA ratio, it is extremely unlikely that LTP is selectively expressed by a potentiation of the AMPAR conductance, or that the observed increase in NMDA/non-NMDA ratio can be accounted for by differences in stimulation intensity between the control and LTP groups.

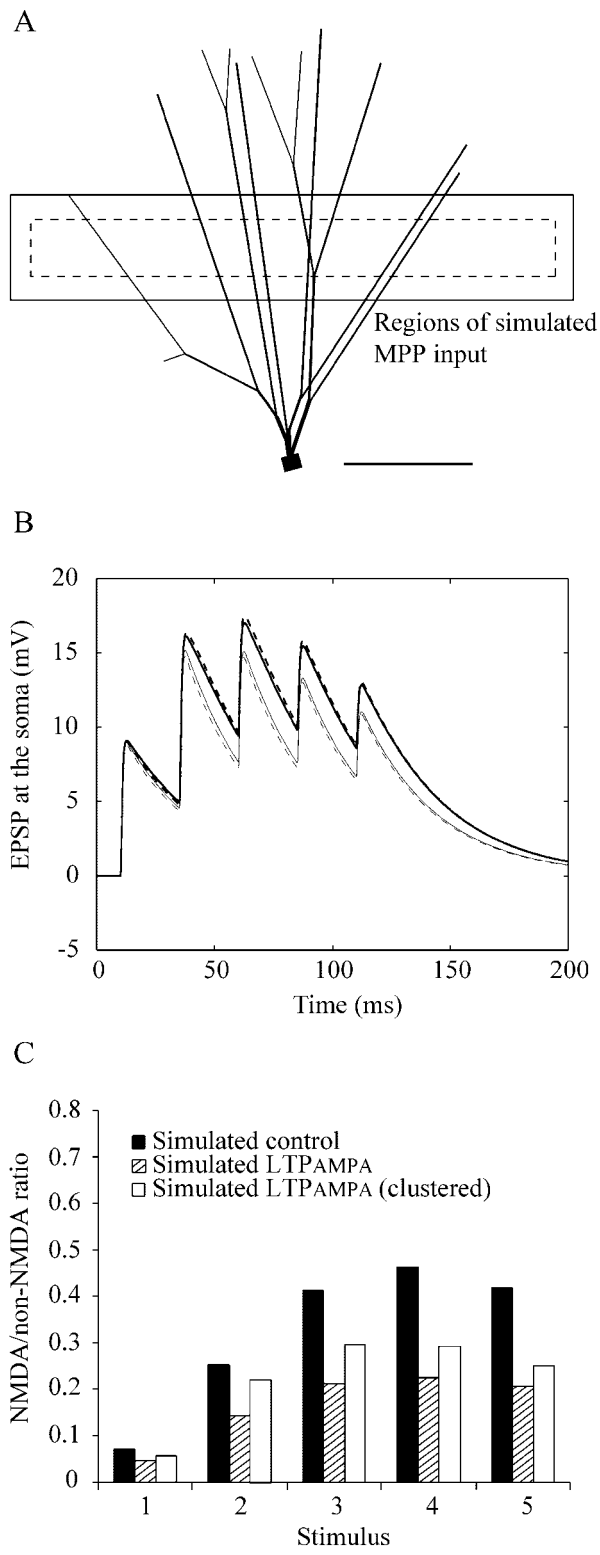

FIGURE 5. Effect of the distribution of activated synapses on the NMDA/non-NMDA ratio. A: Morphology of the model dentate gyrus (DG) granule cell. The solid-line box indicates the dendritic region receiving medial perforant path (MPP) input in the simulations shown in Figure 4. The dashed-line box indicates the region receiving MPP input at lower stimulus intensity. B: The pair of solid-line traces shows the combined (thick) and the non-NMDA component (thin) in LTP_{AMPA} when synapses were distributed over the region in the solid-line box in A. The pair of dashed-line traces shows the combined (thick) and the non-NMDA component (thin) in long-term potentiation $(LTP)_{AMPA}$ when synapses were clustered in the dashed-line box in A. C: Comparison of the NMDA/non-NMDA ratio. In the case of LTP_{AMPA}, the ratio increased when the synapses were clustered, but the ratio was still significantly lower than that of the control simulation. Scale bar = 100 μm in A.

DISCUSSION

Frequency-dependent NMDAR-mediated synaptic transmission in the hippocampus has been studied both in vivo in dentate gyrus (Blanpied and Berger, 1992) and in vitro in CA1 (Collingridge et al., 1988). The temporal summation of EPSPs evoked by burst stimulation of perforant path afferents facilitates activation of NMDARs. In accordance with these prior studies, we observed significant facilitation of the NMDA component in response to stimulation frequencies of 20 Hz and higher. This provided us with a protocol to measure the NMDA component under physiological concentrations of Mg^{2+}; 40 Hz was chosen to avoid induction of LTP.

We employed two procedures to ensure comparable levels of NMDAR activation in control and potentiated cells. First, we controlled the level of depolarization mediated by non-NMDARs. Second, the NMDA/non-NMDA ratio we calculated for comparison between the two groups is equivalent to normalizing the NMDA component to the level of depolarization.

The increase in NMDA/non-NMDA ratio that we observed is consistent with an enhancement of the NMDA component. However, to make inferences about changes in the NMDAR conductance, several factors need to be considered. First, potentiation of non-NMDARs may enhance the NMDA component in a voltage-dependent manner (due to the voltage-dependent blockade of the channel) even without potentiation of NMDARs. Second, the ratio may be changed if the spatial distribution of active synapses differs between the control and potentiated group. We have addressed both of these two issues with computer modeling studies. Simulation results ruled out the possibility of selective potentiation of non-NMDARs. In the worst-case scenario, when only AMPAR-mediated conductance was potentiated and the activated synapses were clustered closer together, the NMDA/non-NMDA ratio was not even equal to the control level, let alone higher than the control

as we observed empirically. Thus, the NMDAR-mediated conductance must be potentiated to account for the increased ratio. It should be noted, however, that our simulation methods do not discriminate between pre- and postsynaptic mechanisms of this potentiation.

Another important issue is that active conductances on the dendrites may contribute to the nonlinear summation of unitary EPSPs (reviewed by Magee et al., 1998; Reyes, 2001) and complicate interpretation of EPSPs recorded at the soma. Dendritic active conductances have not been included in the current model due to a lack of knowledge of their distribution and properties in DG granule cells. In this study, because the level of depolarization was maintained at similar levels in both control and LTP group, the contribution of active conductances in the dendrites can be assumed to be equivalent for both groups.

In an earlier study, Muller et al. (1989) found no potentiation, but a small depression, of the NMDA component of synaptic responses evoked by a short stimulation train after LTP induction. The discrepancy could be due to the time course of the train (four pulses at 100 Hz) Muller et al. used to reveal the NMDA component. Because of their slow kinetics, NMDARs would not be fully activated at the onset of the fourth pulse of the train used by Muller and colleagues, which was 30 ms from the start of the train.

Potentiation of NMDARs is likely to have an impact on the dynamics of synaptic transmission in several ways. First, the Ca^{2+} signal mediated by NMDARs may be enhanced at potentiated synapses, and therefore change the stimulus patterns required to induce LTD or additional LTP, i.e., the dynamics of metaplasticity. Second, enhanced NMDARs could change the mode of spike generation in DG granule cells. Lynch et al. (2000) have demonstrated that transient exposure to Mg^{2+}-free ACSF can cause an increase in the NMDA component and as a consequence shift the cell from a single-spiking to a burst-discharging mode of firing. Third, changes in the NMDA/non-NMDA ratio may influence network properties in a manner that is not readily deduced from studies at the synaptic level. Modeling of the segmental locomotor network in lamprey has shown that the balance between NMDAR and non-NMDAR activation can influence the stability and oscillation frequency of the network (Traven et al., 1993).

In this study, we also investigated the contribution of NMDARs to frequency facilitation, and the possibility that frequency facilitation is modified after LTP induction. Our results showed that NMDARs enhance frequency facilitation of EPSPs evoked by 40-Hz trains. Since NMDARs contribute to the output pattern of hippocampal neurons evoked by high-frequency input, changes in frequency facilitation would be expected if enhancement of NMDARs occurs after LTP. Although our results support the hypothesis that NMDARs are enhanced by LTP, no significant changes in the facilitation pattern were observed. The lack of change in the facilitation pattern is in accordance with studies in the CA1 region (Pananceau et al., 1998; Buonomano, 1999; Selig et al., 1999). The precise expression mechanism of LTP remains unclear. For example, if LTP is partly attributable to an increase in presynaptic release, frequency facilitation would be reduced (Zucker, 1989) which could cancel the enhancing effect of potentiated NMDARs on frequency facilitation.

In summary, we used 40-Hz train stimulation combined with NMDAR antagonist application to measure the NMDA receptor-mediated component of synaptic responses of potentiated and non-potentiated slices. Based on the observed increase in the NMDA/non-NMDA ratio after LTP, we propose that LTP is partially and significantly expressed through enhancement of the NMDAR conductance and have justified our argument with results from computer simulations.

REFERENCES

Aradi I, Holmes WR. 1999. Role of multiple calcium and calcium-dependent conductances in regulation of hippocampal dentate granule cell excitability. J Comput Neurosci 6:215–235.

Bashir ZI, Alford S, Davies SN, Randall AD, Collingridge GL. 1991. Long-term potentiation of NMDA receptor-mediated synaptic transmission in the hippocampus. Nature 349:156–158.

Bayazitov I, Kleschevnikov A. 2000. Afferent high strength tetanizations favour potentiation of the NMDA vs. AMPA receptor-mediated component of field EPSP in CA1 hippocampal slices of rats. Brain Res 866:188–196.

Berger TW. 1984. Long-term potentiation of hippocampal synaptic transmission affects rate of behavioral learning. Science 224:627–630.

Berger TW, Rinaldi PC, Weisz DJ, Thompson RF. 1983. Single-unit analysis of different hippocampal cell types during classical conditioning of rabbit nictitating membrane response. J Neurophysiol 50:1197–1219.

Blanpied TA, Berger TW. 1992. Characterization in vivo of the NMDA receptor-mediated component of dentate granule cell population synaptic responses to perforant path input. Hippocampus 2:373–388.

Bliss TV, Collingridge GL. 1993. A synaptic model of memory: long-term potentiation in the hippocampus. Nature 361:31–39.

Buonomano DV. 1999. Distinct functional types of associative long-term potentiation in neocortical and hippocampal pyramidal neurons. J Neurosci 19:6748–6754.

Claiborne BJ, Amaral DG, Cowan WM. 1990. Quantitative, three-dimensional analysis of granule cell dendrites in the rat dentate gyrus. J Comp Neurol 302:206–219.

Clark KA, Collingridge GL. 1995. Synaptic potentiation of dual-component excitatory postsynaptic currents in the rat hippocampus. J Physiol 482:39–52.

Collingridge GL, Herron CE, Lester RA. 1988. Frequency-dependent N-methyl-D-aspartate receptor-mediated synaptic transmission in rat hippocampus. J Physiol 399:301–312.

Desmond NL, Levy WB. 1984. Dendritic caliber and the 3/2 power relationship of dentate granule cells. J Comp Neurol 227:589–596.

Desmond NL, Levy WB. 1985. Granule cell dendritic spine density in the rat hippocampus varies with spine shape and location. Neurosci Lett 54:219–224.

Herron CE, Lester RA, Coan EJ, Collingridge GL. 1986. Frequency-dependent involvement of NMDA receptors in the hippocampus: a novel synaptic mechanism. Nature 322:265–268.

Hines ML, Carnevale NT. 1997. The NEURON simulation environment. Neural Comput 9:1179–1209.

Kapur A, Lytton WW, Ketchum KL, Haberly LB. 1997. Regulation of the NMDA component of EPSPs by different components of postsynaptic GABAergic inhibition: computer simulation analysis in piriform cortex. J Neurophysiol 78:2546–2559.

Kauer JA, Malenka RC, Nicoll RA. 1988. A persistent postsynaptic modification mediates long-term potentiation in the hippocampus. Neuron 1:911–917.

Kleppe IC, Robinson HP. 1999. Determining the activation time course of synaptic AMPA receptors from openings of colocalized NMDA receptors. Biophys J 77:1418–1427.

Larson J, Lynch G. 1988. Role of N-methyl-D-aspartate receptors in the induction of synaptic potentiation by burst stimulation patterned after the hippocampal theta- rhythm. Brain Res 441:111–118.

Lester RA, Clements JD, Westbrook GL, Jahr CE. 1990. Channel kinetics determine the time course of NMDA receptor-mediated synaptic currents. Nature 346:565–567.

Lynch G, Baudry M. 1984. The biochemistry of memory: a new and specific hypothesis. Science 224:1057–1063.

Lynch M, Sayin U, Golarai G, Sutula T. 2000. NMDA receptor-dependent plasticity of granule cell spiking in the dentate gyrus of normal and epileptic rats. J Neurophysiol 84:2868–2879.

MacDermott AB, Mayer ML, Westbrook GL, Smith SJ, Barker JL. 1986. NMDA-receptor activation increases cytoplasmic calcium concentration in cultured spinal cord neurones. Nature 321:519–522.

Magee J, Hoffman D, Colbert C, Johnston D. 1998. Electrical and calcium signaling in dendrites of hippocampal pyramidal neurons. Annu Rev Physiol 60:327–346.

McNaughton BL, Barnes CA, Andersen P. 1981. Synaptic efficacy and EPSP summation in granule cells of rat fascia dentata studied in vitro. J Neurophysiol 46:952–966.

Muller D, Lynch G. 1988. Long-term potentiation differentially affects two components of synaptic responses in hippocampus. Proc Natl Acad Sci U S A 85:9346–9350.

Muller D, Joly M, Lynch G. 1988. Contributions of quisqualate and NMDA receptors to the induction and expression of LTP. Science 242:1694–1697.

Muller D, Larson J, Lynch G. 1989. The NMDA receptor-mediated components of responses evoked by patterned stimulation are not increased by long-term potentiation. Brain Res 477:396–399.

Nowak L, Bregestovski P, Ascher P, Herbet A, Prochiantz A. 1984. Magnesium gates glutamate-activated channels in mouse central neurones. Nature 307:462–465.

O'Connor JJ, Rowan MJ, Anwyl R. 1995. Tetanically induced LTP involves a similar increase in the AMPA and NMDA receptor components of the excitatory postsynaptic current: investigations of the involvement of mGlu receptors. J Neurosci 15:2013–2020.

Ozawa S, Kamiya H, Tsuzuki K. 1998. Glutamate receptors in the mammalian central nervous system. Prog Neurobiol 54:581–618.

Pananceau M, Chen H, Gustafsson B. 1998. Short-term facilitation evoked during brief afferent tetani is not altered by long-term potentiation in the guinea-pig hippocampal CA1 region. J Physiol (Lond) 508:503–514.

Perkel DJ, Nicoll RA. 1993. Evidence for all-or-none regulation of neurotransmitter release: implications for long-term potentiation. J Physiol 471:481–500.

Reyes A. 2001. Influence of dendritic conductances on the input-output properties of neurons. Annu Rev Neurosci 24:653–675.

Selig DK, Nicoll RA, Malenka RC. 1999. Hippocampal long-term potentiation preserves the fidelity of postsynaptic responses to presynaptic bursts. J Neurosci 19:1236–1246.

Traven HG, Brodin L, Lansner A, Ekeberg O, Wallen P, Grillner S. 1993. Computer simulations of NMDA and non-NMDA receptor-mediated synaptic drive: sensory and supraspinal modulation of neurons and small networks. J Neurophysiol 70:695–709.

West MO, Christian E, Robinson JH, Deadwyler SA. 1981. Dentate granule cell discharge during conditioning. Relation to movement and theta rhythm. Exp Brain Res 44:287–294.

Wood ER, Dudchenko PA, Robitsek RJ, Eichenbaum H. 2000. Hippocampal neurons encode information about different types of memory episodes occurring in the same location. Neuron 27:623–633.

Xiao MY, Niu YP, Wigstrom H. 1996. Activity-dependent decay of early LTP revealed by dual EPSP recording in hippocampal slices from young rats. Eur J Neurosci 8:1916–1923.

Xie X, Berger TW, Barrionuevo G. 1992. Isolated NMDA receptor-mediated synaptic responses express both LTP and LTD. J Neurophysiol 67:1009–1013.

Zucker RS. 1989. Short-term synaptic plasticity. Annu Rev Neurosci 12:13–31.